IOPscience iopscience.iop.org

Home Search Collections Journals About Contact us My IOPscience

Diffusion controlled grain growth in primary crystallization: Avrami exponents revisited

This article has been downloaded from IOPscience. Please scroll down to see the full text article.

1998 J. Phys.: Condens. Matter 10 3833

(http://iopscience.iop.org/0953-8984/10/17/014)

View the table of contents for this issue, or go to the journal homepage for more

Download details:
IP Address: 171.66.16.151
The article was downloaded on 12/05/2010 at 23:22

Please note that terms and conditions apply.

J. Phys.: Condens. Matter **10** (1998) 3833–3844. Printed in the UK PII: S0953-8984(98)89567-2

Diffusion controlled grain growth in primary crystallization: Avrami exponents revisited

T Pradell†, D Crespo‡, N Clavaguera§ and M T Clavaguera-Mora‖

† ESAB, Universitat Politècnica de Catalunya, Urgell 187, 08036 Barcelona, Spain
‡ Departament de Física Aplicada, Universitat Politècnica de Catalunya, Campus Nord UPC, Mòdul B4, 08034 Barcelona, Spain
§ Física de l'Estat Sòlid, Facultat de Física, Universitat de Barcelona, Diagonal 647, 08028 Barcelona, Spain
‖ Grup de Física de Materials I, Departament de Física, Universitat Autònoma de Barcelona, 08193 Bellaterra, Spain

Received 26 November 1997

Abstract. The anomalous behaviour of the Avrami exponents found in the primary crystallization of amorphous alloys leading to nanostructured materials is considered. A kinetic model able to adequately treat such phase transformation has been formulated by means of the implementation of a soft-impingement diffusion mechanism after a transient interface controlled growth. A decrease in the nucleation rate as crystallization proceeds has also been considered. Comparison of the model with experimental data is performed, giving excellent agreement. The soft-impingement diffusion mechanism is demonstrated to be responsible for the anomalous behaviour of the Avrami exponent, the decreasing nucleation rate being a second-order effect.

1. Introduction

Experimental data on kinetics of primary crystallization often deviate from the theory of Kolmogorov–Johnson–Mehl–Avrami (KJMA) [1–3], specially in the late stages of crystallization. However, statistical considerations underlying KJMA may be applicable to this situation, and the challenge is to find suitable models for the nucleation and growth rates in order to obtain an adequate description of the experimental data.

One of the parameters commonly evaluated for analysing experimental data which follow KJMA kinetics is the well known Avrami exponent, which is used as a tracer of the mechanisms underlying the transformation. Dependence of nucleation and growth rates on temperature and time are both responsible for the Avrami exponent determined, and, although experimental procedures provide some knowledge of these dependencies, the same values of the Avrami exponents may be obtained as a result of different mechanisms. Usually, several externally controlled thermal conditions are used in order to obtain overall information on the microstructural development through the evaluation of the crystalline fraction evolution or the Avrami exponent. Therefore, an adequate theoretical description is necessary to fit the time evolution of the crystalline fraction, $x(t)$, and to obtain an adequate interpretation of the values of the Avrami exponent, $n(t)$.

One of the situations where the misfit between KJMA and experimental data is observed is the primary crystallization of amorphous alloys. Evaluation of Avrami exponents from $x(t)$ in such processes usually results in abnormally low values, which have given rise to

0953-8984/98/173833+12$19.50 © 1998 IOP Publishing Ltd

some controversy and confusion in the literature [4–8]. Recently, experimental data on the crystalline fraction evolution of BCC Fe(Si) with a DO_3 structure precipitation in a FINEMET alloy has been modelled by considering homogeneous nucleation and interface plus diffusion controlled grain growth with interference of the diffusion profiles between neighbour grains [9, 10], giving an excellent agreement with experimental data.

The main feature of the model is the introduction of a microstructural dependence of the grain growth, as a consequence of grain interaction typical of partitioning transformations where the precipitate has a different composition from the matrix in which it develops. Normally, partitioning transformations result in the presence of gradients of the concentrations of several solutes at the edge of the grains, the growth rate being limited by the slowest-diffusing specimen [11]. However, as crystallization proceeds the diffusion profiles of neighbour grains begin to overlap to an appreciable extent (soft impingement), giving rise to a further decrease in the growth rate because of the reduction in the concentration gradient [9]. Therefore, the model referred to may adequately treat the growth problem limited by soft impingement in primary crystallizations. However, a decreasing nucleation rate should also be expected in such transformations, since the composition of the matrix changes as crystallization proceeds, resulting in a remaining amorphous phase stable versus crystallization. Therefore, the effect of decreasing nucleation rates should also be considered and compared with the effect of the growing mechanism in the resulting kinetics.

In this paper the Avrami exponent is calculated with the model of growth referred to above for a primary crystallization.The effect of introducing the interference of the already developed microstructure on the grain growth is shown. Moreover, the effect of the decrease in the nucleation rate expected in such transformations is also considered. The relative importance of the decrease of the growth rate and of the nucleation rate during the transformation is discussed by comparison with experimental data, and their implications on the determined values of the Avrami exponent are discussed.

2. Evaluation of Avrami exponents

The kinetics of first-order phase transitions driven by nucleation and growth kinetics is statistically described by the KJMA theory. The Avrami equation relates the evolution of crystallized fraction $x(T, t)$ to the extended crystallized fraction $\tilde{x}(T, t)$ by

$$\frac{\mathrm{d}x(T,t)}{1-x(T,t)} = \mathrm{d}\tilde{x}(T,t) \tag{1}$$

where T accounts not only for the temperature but also for any other external variables characterizing the process, and t is time. Therefore, the transformed volume fraction may be evaluated as

$$x(T,t) = 1 - \exp(-\tilde{x}(T,t)). \tag{2}$$

The extended volume fraction may easily be calculated from the kinetic parameters as

$$\tilde{x}(T,t) = \int_0^t I(T,\tau)V(T,\tau,t)\,\mathrm{d}\tau = \int_0^t I(T,\tau)\,f_d[r(T,\tau,t)]^d\,\mathrm{d}\tau \tag{3}$$

where I is the nucleation rate, $V(T, \tau, t)$ is, at time t, the d-dimensional volume of a grain born at time τ, and consequently $r(T, \tau, t)$ is its radius and f_d is the d-dimensional form factor.

The Avrami exponent is defined from the slope of $\ln(\tilde{x}(T, t))$ versus $\ln(t)$,

$$n(T,t) = \frac{\mathrm{d}[\ln(-(\ln(1-x(T,t))))]}{\mathrm{d}[\ln(t)]} = \frac{\mathrm{d}[\ln(\tilde{x}(T,t))]}{\mathrm{d}[\ln(t)]} \tag{4}$$

and it is evaluated only in the case of isothermal crystallizations; therefore, T becomes a fixed parameter.

The radius $r(T, \tau, t)$ is obtained by integration of the growth rate $G(T, t)$. Then, for instance, for a constant nucleation and any radius dependent grain growth, $G(T, r(\tau, t))$, the radius has the form $r(T, \tau, t) = G_0(T)(t - \tau)^q$, and the extended transformed fraction and the Avrami exponent become, respectively,

$$\tilde{x}(T, t) = \frac{1}{(qd + 1)} I_0 f_d G_0^d t^{qd+1}$$
$$n = qd + 1. \tag{5}$$

If the time dependence is the same during the whole crystallization process, that is to say, if there is no change in the mechanism of transformation, the Avrami exponent should be constant throughout the whole process. The case of increasing and decreasing nucleation rates may also be considered, taking, for instance, $I(T, \tau) = I_0(T)\tau^p$ and $I(T, \tau) = I_0(T)(a + \tau)^{-p}$ respectively. In that case the Avrami exponents are not constant but continuously increase or decrease, and give at the end of the transformation $n(t \to \infty) \to p + qd + 1$ for the case of increasing nucleation rates, and $n(t \to \infty) \to qd$ for the case of decreasing nucleation rates. This is a general result for any kind of time dependency of the nucleation rate [12]. As a consequence, decreasing or increasing nucleation rates are often considered to be responsible for non-constant Avrami exponents.

In the case of interface controlled growth the growth rate is constant and the Avrami exponent becomes equal to $d + 1$, namely 4 for three-dimensional growth (with constant nucleation rate), 3 for two-dimensional growth and so on.

For diffusion controlled growth rate, when steady state conditions are reached we have [11]

$$G(T, r) = \frac{\mathrm{d}r}{\mathrm{d}t} = \frac{D_0(T)}{r} \tag{6}$$

which can be integrated obtaining

$$r(t, \tau) = 2[D_0(T)(t - \tau)]^{1/2} \tag{7}$$

thus leading to a value of $1 + d/2$ for the Avrami exponent (with constant nucleation rate), and in particular $5/2$ for the three-dimensional growth. Moreover, in the case of primary transformations where a three-dimensional diffusion controlled growth rate is expected, the minimum value expected even for decreasing nucleation rates is $qd = 3/2$.

Finally, for the case of a decreasing growth rate with constant nucleation rate, the minimum value expected for the Avrami exponent is 1. Values of the Avrami exponent below this figure are thus classically attributed to both decreasing nucleation and growth rates.

3. Diffusion controlled grain growth in a primary crystallization

The above discussion is very fruitful for understanding complex crystallization processes. To illustrate this we will now focus the discussion on the nanocrystallization of a FINEMET alloy. These materials have been extensively studied from several points of view: their good soft magnetic properties [13], the effect of alloy composition on their properties [14], kinetics of crystallization [6, 7, 9, 10, 15, 16] and crystalline and amorphous characterization [4, 16–18]. In particular we will analyse the isothermal nanocrystalline precipitation of a BCC ($Fe_{78}Si_{22}$) phase, with a DO_3 defective in Si superstructure, in a FINEMET material of composition $Fe_{73.5}Si_{17.5}CuNb_3B_5$. Careful kinetic analysis by differential scanning

calorimetry (DSC) and Mössbauer spectroscopy (MS) [16] has demonstrated that the isothermal crystallization process of FINEMET materials shows a two-step process: a first process, which is not related to crystalline precipitates but rather to a change in the short-range order of the amorphous phase associated to an enhancement of the hyperfine magnetic interaction (Cu is separated from the amorphous matrix forming clusters); and a second process which corresponds to the primary precipitation itself. These two processes may be detected by DSC analysis under isothermal or continuous heating conditions. Figure 1(a) shows the isothermal calorimetric signal, which is formed by the addition of two signals corresponding to the two processes already mentioned, the first process shown in figure 1(b) and the second process shown in figure 1(c). This two-step process is also observed under continuous-heating conditions, where the first process appears as a broad peak at lower temperatures than the primary precipitation and may be eliminated by a first thermal treatment at temperatures of about 430 °C [18].

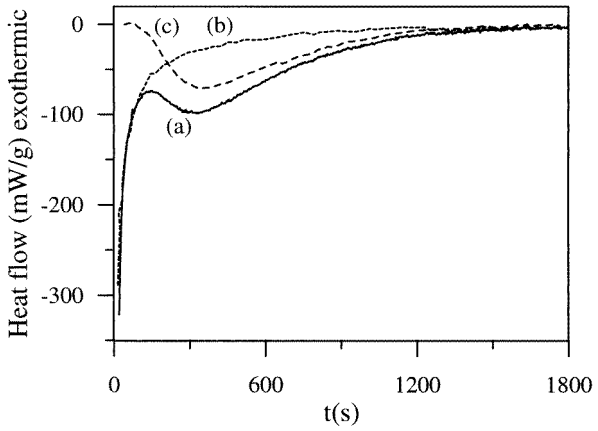

Figure 1. (a) Isothermal DSC signal at 763 K corresponding to $Fe_{73.5}Si_{17.7}CuNb_3B_5$; the two-step process is formed by a continuous decaying signal (b) and crystallization peak (c).

The analysis of the isothermal data in order to obtain the transformed fraction and the Avrami exponent will be performed on the isothermal calorimetric signal after elimination of the first process. Therefore, the effect of Cu clustering will be eliminated from the analysis of the nanocrystalline precipitation. Moreover, a diffusion controlled growth will dominate the transformation as the primary phase has a different composition from the amorphous phase. The chosen FINEMET composition has the advantage that the nanocrystalline precipitate has an Fe/Si ratio very close to the one corresponding to the original amorphous alloy and which, under isothermal conditions, does not change as crystallization proceeds [16]. In that case, mostly Nb will diffuse out of the nanocrystalline phase. Other FINEMET compositions poorer in Si will show a more complicated behaviour [18].

Figure 2(a) shows the comparison of the experimentally determined transformed fraction with the computed values, considering constant nucleation and either interface or diffusion controlled growth, according to [9] and [10]. Figure 2(b) shows the experimentally determined Avrami exponents compared to the computed values for both kinetics. The experimental Avrami exponents appear to be close to 4 at the beginning of the transition, and further decrease below the values predicted for a diffusion controlled transition. A common explanation associates this behaviour with a decreasing nucleation rate during the transformation. A decreasing nucleation rate is expected because in a primary transformation

the change of the composition of the amorphous matrix results in a change of the thermodynamic factors which favour the initial nucleus precipitation. In order to take this effect into account the first mean-field approximation is to suppose a linear decreasing nucleation rate as $I(T,\tau) = I_0(T)(1 - x(\tau))$ [10]. Figure 2 also shows the result of introducing the linear decreasing nucleation rate to the diffusion controlled grain growth expected in a such transformation. None of these models seems able to explain the experimental behaviour. We will demonstrate that the consideration of a diffusion controlled growth with soft impingement will explain the behaviour of the Avrami exponents and the transformation curves without introducing a decreasing nucleation rate. Furthermore, the introduction of a decreasing nucleation will result in a second-order effect.

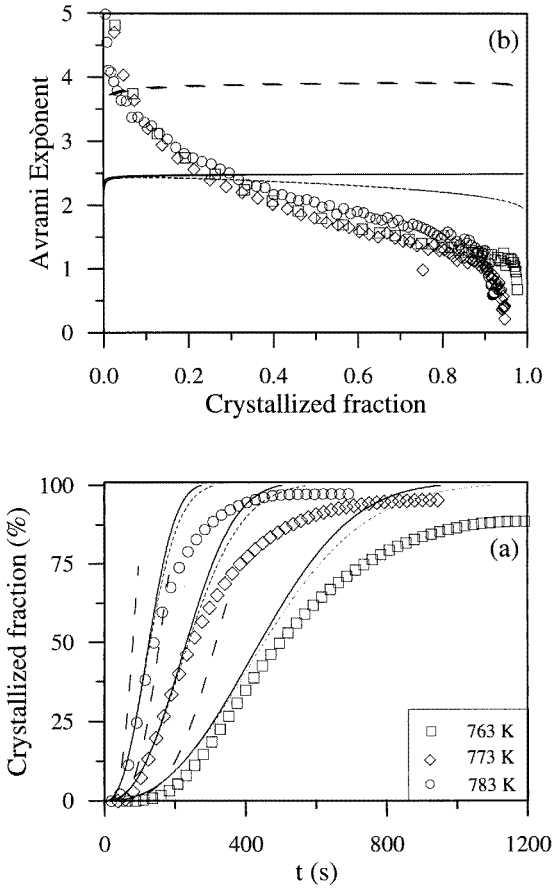

Figure 2. (a) Experimental transformed fraction versus time and (b) experimentally determined Avrami exponents versus crystallization fraction compared to computed interface controlled (dashed line) and diffusion controlled (solid line) growth.

The first consideration that should be made is that equation (6) describes the diffusion controlled growth rate of the grain after steady conditions have been achieved, thus neglecting the initial stage leading to the steady state regime. In a simplified view, one can consider that nuclei are formed by fluctuations in the disordered phase and, at the initial stage of growth, the species rejected from the crystalline phase will pile up ahead

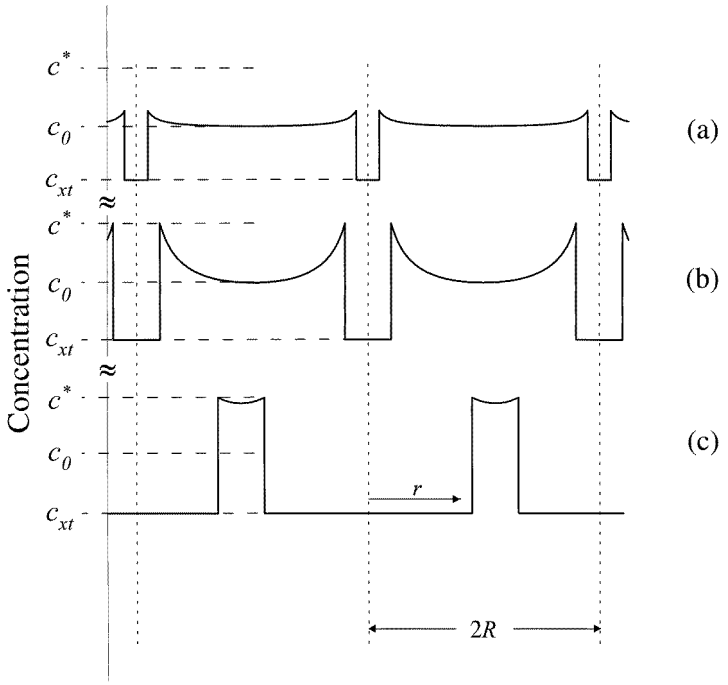

Figure 3. Sketch of the evolution of the concentration of the diffusion species as the transformation advances. (a) Transient growth process. (b) Diffusion controlled growth under steady state conditions. (c) End of transformation while $c \to c^*$.

of the interface until metastable local equilibrium is reached, as shown in figure 3(a), (b). There are several effects which determine the value of the initial growth rate, such as the critical size of the nuclei, r^*, the Gibbs–Thompson effect, the balance between interface and diffusion until diffusion becomes the limiting mechanism etc. However, since we are using a mean-field theory to analyse the overall transformation, in our simplified model we will consider that growth is interface controlled until a threshold radius, r_T, is attained. Therefore, in order to describe the growth habit more accurately, the growth rate is taken as

$$\frac{\mathrm{d}r}{\mathrm{d}t} = \begin{cases} u(T) & r \leqslant r_T \\ \dfrac{D(T)}{r}\dfrac{C^* - C}{C^* - C_{xt}} & r > r_T \end{cases} \tag{8}$$

where C_{xt}, C^* and C are respectively the concentrations of the slowest-moving species inside the grain, at the grain boundary and far from the grain (see figure 3). The diffusion controlled growth rate corresponds to an isolated grain with spherical symmetry, according to [11], and $D(T)$ accounts for a diffusion coefficient given by $D(T) = D_\infty \mathrm{e}^{-(E_D/kT)}$. The value of r_T is obtained by imposing continuity in radius size, giving $r_T = (D(T)/u(T))(C^* - C/C^* - C_{xt}) - r^*$. This approach will produce a discontinuous growth rate transition at r_T, but it does not seriously affect the results [9] and is easily introduced in the calculation.

Equation (8) means that the growth rate of an isolated grain depends on the concentration value far from the grain. As a first approximation, we can ignore the effect of the rest of the growing grains on this value, and thus take $C = C_0$, the concentration of the diffusing

element in the matrix at $t = 0$ (see figure 3(b)). This first approximation is usually known as diffusion controlled growth with *hard impingement*.

The validity of this approximation essentially depends on the difference $C^* - C$. If this difference is large, the excess (or defect) of the species in the untransformed phase will affect the growth rate very little. However, the presence of solute in the matrix due to the growth of neighbour grains will reduce this difference and, at the end of the transformation, it is likely that $C^* - C \to 0$. This fact is also sketched in figure 3, where the reduction in the concentration gradient at the grain boundary is shown. Then, as a second approximation, we can consider the variation in C while the transformation proceeds, an approximation known as *soft-impingement diffusion*.

The determination of C in (8) is obtained by considering the average mean value of the concentration of solute in the remaining matrix, which can be evaluated by writing a mass balance

$$\gamma x(t) C_{xt} + (1 - \gamma x(t)) C = C_0 \tag{9}$$

where γ accounts for the crystallized fraction at the end of the primary crystallization ($x = 1$). Imposing that $C(t \to \infty) \to C^*$, expression (9) becomes the level rule, namely,

$$\frac{\gamma}{1 - \gamma} = \frac{C^* - C_0}{C_0 - C_{xt}}. \tag{10}$$

Finally, substituting (9) and (10) into (8) we obtain

$$\frac{\mathrm{d}r}{\mathrm{d}t} = \begin{cases} u(T) & r \leqslant r_T \\ \dfrac{D_0(T)}{r} \varphi(x(t)) & r > r_T \end{cases} \tag{11}$$

where $D_0(T) = D(T)(C^* - C_0)/(C^* - C_{xt}) = \gamma D(T)$ and $-\varphi(x(t)) = 1$ for hard impingement and $\varphi(x(t)) = [1 - x(t)]/[1 - \gamma x(t)]$ for soft impingement. Note that new adjustable parameters are not introduced in the soft impingement approach if γ can be determined independently.

Finally, the change of the matrix composition along the transformation is also expected to result in a change of the nucleation rate. In the nanocrystalline precipitation of the FINEMET alloy the matrix enriches in Nb as transformation proceeds. Nb is a well known stabilizer of the amorphous phase, and therefore a reduction of the nucleation rate should be expected. As a first mean-field approximation, the reduction may be taken as $I(T, \tau) = I_0(T)(1 - x(\tau))$ [10].

We will apply this model also to the FINEMET—$Fe_{73.5}Si_{17.5}CuNb_3B_5$—nanocrystallization of a BCC ($Fe_{78}Si_{22}$) primary phase, where Mössbauer measurements show that the transformed fraction at the end of the primary crystallization is about 60% [16], which gives a value of $\gamma = 0.6$.

Figures 4(a) and 5(a) show the experimentally measured transformed fraction versus time compared with the interface plus diffusion controlled growth by hard or soft impingement and constant or decreasing nucleation rates. One can see that both approaches describe the beginning of the transformation quite accurately. However, experimental data delay noticeably from the hard-impingement model after the crystallized fraction reaches about 50%. Moreover, the decreasing nucleation rates for both growing process produce an extra delay of the transformed fraction. However, the effect is much smaller than the soft-impingement consideration, and in itself is not able to explain the experimental behaviour. Agreement between the soft-impingement approximation and experimental data is excellent, always allowing for the uncertainty of the experimental data.

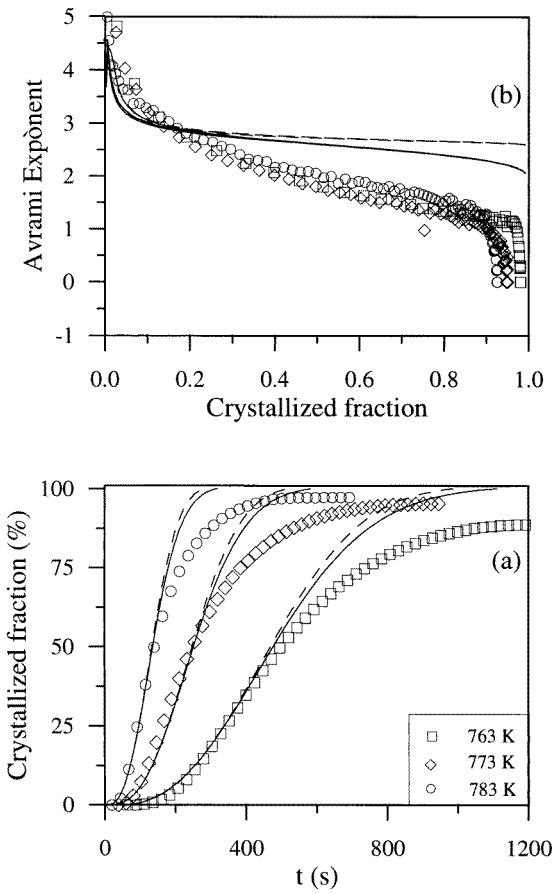

Figure 4. (a) Transformed fraction versus time and (b) Avrami exponent versus crystallized fraction. Comparison of experimental data with computed values in the hard-impingement diffusion approximation with constant (dashed line) and decreasing (solid line) nucleation rates.

Avrami exponents give an alternative view of this agreement. Figures 4(b) and 5(b) show the experimentally determined Avrami exponents compared to the computed values for the hard or soft impingement and constant or decreasing nucleation rates. Remembering that the beginning of the grain growth is interface controlled in both cases, it is possible to understand the present agreement between experimental and computed values at early stages of crystallization. However, in the hard-impingement model the Avrami exponent tends to a final value of $5/2$, as predicted theoretically in a diffusion controlled growth process, far from the experimentally determined values. On the other hand, the soft-impingement model follows the evolution of the experimental data more closely, the reduction in the diffusion gradient being responsible for the low values of the Avrami exponent observed at the end of the transformation.

These final values show a surprising behaviour, namely they go below 1. This result was previously obtained in the literature, and the usual explanation was that the nucleation rate decreased at late stages of the transition [4, 6, 19]. We see in the analysed case that a decreasing nucleation rate produces an extra decrease of the Avrami exponents, but this in itself is not able to explain the general behaviour of the data (figure 5). In our model we

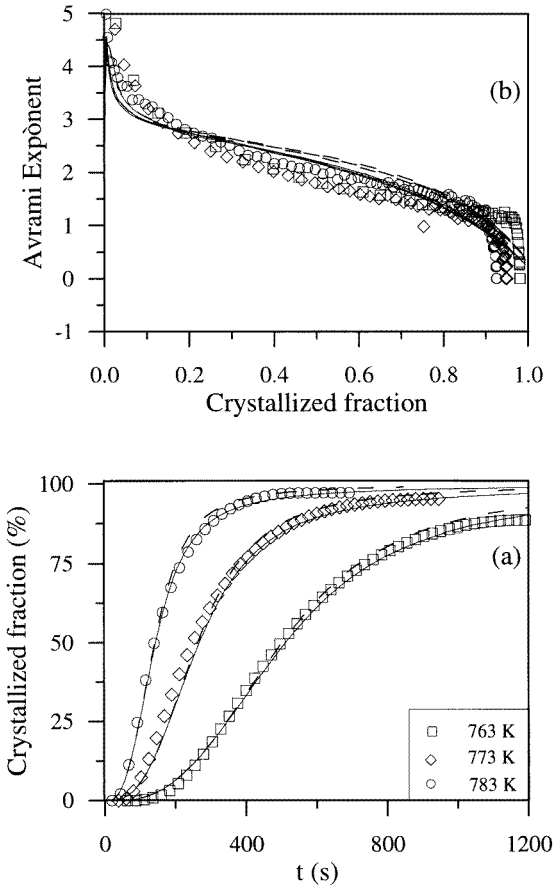

Figure 5. (a) Transformed fraction versus time and (b) Avrami exponent versus crystallized fraction. Comparison of experimental data with computed values in the soft-impingement diffusion approximation with constant (dashed line) and decreasing (solid line) nucleation rates.

have also considered constant nucleation rate, and the computed values go below 1. In fact, considering the case where growth is stopped when the transformed fraction has reached a value close to 1 and only nucleation remains, we can write the extended fraction at time $t + \Delta t$ as a function of $\tilde{x}(t)$

$$\tilde{x}(t + \mathrm{d}t) = \tilde{x}(t) + IV_\varepsilon \Delta t \tag{12}$$

where V_ε is the volume of a nucleus. Thus evaluation of equation (5) gives

$$n(t + \Delta t) \approx \frac{IV_\varepsilon t}{\tilde{x}(t) + IV_\varepsilon \Delta t} \approx \frac{IV_\varepsilon t}{\tilde{x}(t)} \tag{13}$$

because $IV_\varepsilon \Delta t$ is negligible with respect to $\tilde{x}(t)$. This leads to a shocking result, namely that the classically expected value of $n = 1$ can only be obtained if $\tilde{x}(t) \approx IV_\varepsilon t$, which means that the growth contribution to the extended fraction is negligible with respect to the nucleation contribution *throughout the whole transformation*. Otherwise, the assumption that $t \to \infty$ is not applicable here because $\tilde{x}(t)$ is an infinity of higher order than $IV_\varepsilon t$ and $n \ll 1$. This means that, contrary to common assumptions, even with a constant nucleation rate the value of the Avrami exponent at the end of the transformation may go below 1.

The above-mentioned result seems to contradict the classical definition of the Avrami exponent as $n(t \to \infty) \to qd + p + 1$ or $n(t \to \infty) \to qd$ for increasing and decreasing nucleation rates, respectively. However, this shows that the classical interpretation of the Avrami exponent is only appropriate if the driving mechanisms do not change over the whole transformation; otherwise an adequate knowledge of the underlying kinetics is needed in order to obtain proper conclusions from the study of the Avrami exponents.

Our results show that, provided 3D growth occurs, the effect of the nucleation and the growth rate in the behaviour of the Avrami exponent is always of a different order of magnitude. The Avrami exponent is always dominated by the growth rate, and the nucleation rate is always a second-order perturbation. The only case where the nucleation rate dominates the behaviour of the Avrami exponent is when the growth rate is negligible during the whole transformation. Even for the particular case of the FINEMET primary transformation, which has a very high nucleation rate, the growth rate is negligible only at the very end of the transformation and therefore it dominates the local value of the Avrami exponent along the transformation.

The results obtained for the FINEMET primary crystallization may also be compared with the ones obtained in the literature. However, although performing continuous heating experiments is a common tool, the special difficulty of obtaining isothermal calorimetric curves means that there are very few papers with such analysis. Moreover, the Avrami exponents have been obtained in very few cases [4–8]. A comparative study of alloys with compositions $Fe_{77.5}Si_{13.5}B_9$, $Fe_{74.5}Si_{13.5}B_9Nb_3$, $Fe_{76.5}Si_{13.5}B_9Cu$ and $Fe_{74.5}Si_{13.5}B_9Nb_3Cu$ has been performed by Zhou *et al* [5], in order to evaluate the effect of Cu and Nb additions to the original Fe–Si–B alloy. In general terms, two types of isothermal curve are obtained, mainly symmetric and asymmetric with long tails, as shown in figure 6. The long tails of the asymmetric curves are related to a diffusion controlled growth and appear for the alloys $Fe_{77.5}Si_{13.5}B_9$, $Fe_{76.5}Si_{13.5}B_9Cu$ and $Fe_{74.5}Si_{13.5}B_9Nb_3Cu$, and the symmetric curve typical of interface controlled growth for the alloy $Fe_{74.5}Si_{13.5}B_9Nb_3$. This seems to contradict our assumption that Nb is responsible for the diffusion controlled process. However, the data have to be considered carefully: for $Fe_{77.5}Si_{13.5}B_9$, $Fe_{76.5}Si_{13.5}B_9Cu$ and $Fe_{74.5}Si_{13.5}B_9Nb_3Cu$ there is a primary crystallization, while in the case of $Fe_{74.5}Si_{13.5}B_9Nb_3$ alloy a eutectic crystallization is obtained. The diffusion controlled grain growth is only obtained as a result of a primary precipitation, while in the case of the eutectic crystallization the growth rate is interface controlled. The fact that even without containing Nb the curves show the typical asymmetric behaviour must be attributed in this case to the fact that the original composition of the alloy is poorer in Si (13.5 at.% Si) than our FINEMET (17.5 at.% Si), and considering that for these alloys the BCC phase formed has also a Si content of about 20 at.% [4, 13], Fe also has to diffuse.

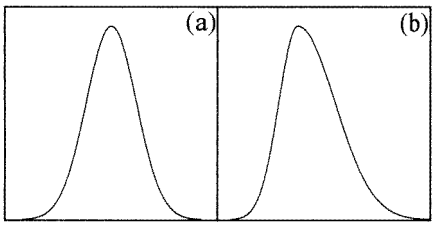

Figure 6. Isothermal calorimetric curves obtained: (a) symmetric for interface controlled growth and (b) asymmetric for diffusion controlled growth.

Moreover, the beginning of the isothermal calorimetric curves has been cut in [5], preventing the observation of the overlap of the calorimetric signal corresponding to Cu clustering, and giving rise to misleading Avrami exponents at the beginning of the transformation.

Therefore, the analysis of the Avrami exponents reported for those materials must take into account the cut-off at the beginning of the transformation and the experimental error of the calorimetric curves at the end of the transformation. Those considerations show that the values obtained for the primary precipitations decrease continuously as crystallization proceeds, and go below $5/2$, while for the eutectic crystallization the Avrami exponent remains more or less constant, and close to 4.

Other measurements of Avrami exponents in FINEMET alloys show in all cases decreasing values as crystallization proceeds [8], and abnormally low values at the end of the transformation ($\sim$0.3 [4], $\sim$0.2 [6] and $\sim$0.7 [7]). Those results agree with the model of a diffusion controlled growth with soft-impingement.

4. Conclusions

The Avrami exponent has been used in the interpretation of experimental data corresponding to the primary crystallization of an amorphous alloy. The implementation of a soft-impingement diffusion mechanism after a transient interface controlled growth to explain a primary crystallization enabled us to fit both the transformed fraction and the Avrami exponent behaviour over the whole transformation. The consideration of decreasing nucleation rates also has physical reasons. However, its effect in the kinetics is a second-order effect compared with the growth mechanism, which has been demonstrated to be chiefly responsible for the experimental behaviour.

The final values of the Avrami exponents, both experimental and computed even with constant nucleation rate, go below 1, in contradiction to the usual hypothesis that a decreasing nucleation rate is needed to understand this kind of behaviour. This result shows that the Avrami exponents are always dominated by the growth rate behaviour, and that the effect of the nucleation rate is a second-order effect.

Acknowledgments

This work was financed by CICYT, grants PB94-1209 and MAT96-0692, UPC, grant PR9505, and Generalitat de Catalunya, grant 1995SGR 00514.

References

[1] Kolmogorov A N 1937 *Bull. Acad. Sci. USSR, Phys. Ser.* **1** 355
[2] Johnson W A and Mehl P A 1939 *Trans. Am. Inst. Mining Metall. Eng.* **135** 416
[3] Avrami M 1939 *J. Chem. Phys.* **7** 1103
Avrami M 1940 *J. Chem. Phys.* **8** 212
Avrami M 1941 *J. Chem. Phys.* **9** 177
[4] Hampel G, Pundt A and Hesse J 1992 *J. Phys.: Condens. Matter* **4** 3195
[5] Zhou F, He K, Sui M and Lai Z 1994 *Mater. Sci. Eng.* A **181/182** 1419
[6] Cserei A, Jiang J, Aubertin F and Gonser U 1994 *J. Mater. Sci.* **29** 1213
[7] Danzig A, Mattern N and Doyle S 1995 *Nucl. Instrum. Methods Phys. Res.* B **97** 465
[8] Liu T, Chen N, Xu Z X and Ma R Z 1996 *J. Magn. Magn. Mater.* **152** 365
[9] Crespo D, Pradell T, Clavaguera-Mora M T and Clavaguera N 1997 *Phys. Rev.* B **55** 3435

[10] Clavaguera N and Clavaguera-Mora M T 1996 *Thermodynamics and Kinetics of Phase Transformations (Mater. Res. Soc. Symp. Proc. 398)* ed J S Im, B Park, A L Greer and G B Stephenson (Pittsburg, PA: Materials Research Society) p 319
[11] Christian W 1975 *The Theory of Transformations in Metals and Alloys* (Oxford: Pergamon)
[12] Pradell T, Crespo D, Clavaguera N and Clavaguera-Mora M T 1997 *Non-Crystalline and Nanoscale Materials: Proc. 5th Int. Workshop on Non-Crystalline Solids* ed J Rivas and M A López-Quintela (Singapore: World Scientific) at press
[13] Yoshizawa Y, Oguma S and Yamauchi K 1988 *J. Appl. Phys.* **64** 6044
Müller M, Mattern N and Illgen L 1992 *J. Magn. Magn. Mater.* **112** 263
Herzer G 1993 *Phys. Scr.* T **4** 307
Schulz R, Trudeau M L, Dussault D, Neste A V and Bailey L D 1994 *Mater. Sci. Eng.* A **179/180** 516
Sakurai M, Matsura M, Kim S H, Yoshizawa Y, Yamauchi K and Suzuki K 1994 *Mater. Sci. Eng.* A **179/180** 469
[14] Kataoka N, Inoue A, Masumoto T, Yoshizawa Y and Yamauchi K 1989 *Japan. J. Appl. Phys.* **28** L1820
Fujinami M, Hashiguchi Y and Yamamoto T 1990 *Japan. J. Appl. Phys.* **29** L477
Yoshizawa Y, Bizen Y and Arakawa S 1994 *Mater. Sci. Eng.* A **179/180** 871
[15] Duhaj P, Svec P, Janickovic D and Matko I 1991 *Mater. Sci. Eng.* **133** 398
Kulik T 1992 *Mater. Sci. Eng.* A **159** 95
Clavaguera N, Pradell T, Zhu J and Clavaguera-Mora M T 1995 *Nanostruct. Mater.* **6** 453
[16] Pradell T, Clavaguera N, Zhu J and Clavaguera-Mora M T 1995 *J. Phys.: Condens. Matter* **7** 4129
[17] Rixeckert G, Schaaf P and Gonser U 1992 *J. Phys.: Condens. Matter* **4** 10 295
Miglierini M 1994 *J. Phys.: Condens. Matter* **6** 1431
[18] Pradell T, Zhou J, Clavaguera N and Clavaguera-Mora M T 1998 *J. Appl. Phys.* **83** (10)
[19] Cahn J W 1996 *Thermodynamics and Kinetics of Phase Transformations (Mater. Res. Soc. Symp. Proc. 398)* ed J S Im, B Park, A L Greer and G B Stephenson (Pittsburg, PA: Materials Research Society)